Superstructure formation of large organic adsorbates on a metal surface: A systematic approach using oligothiophenes on Ag(111)

A. Soukopp, K. Glöckler, P. Kraft, S. Schmitt, M. Sokolowski,* and E. Umbach
Experimentelle Physik II, Universität Würzburg, Am Hubland, D-97074 Würzburg, Germany

E. Mena-Osteritz and P. Bäuerle
Abteilung Organische Chemie II, Universität Ulm, Albert-Einstein-Allee 11, D-89081 Ulm, Germany

E. Hädicke
BASF Aktiengesellschaft, Kunstofflaboratorium, D-67056 Ludwigshafen, Germany
(Received 5 December 1997)

A series of ''end-capped'' oligothiophenes ECnT with different chain lengths n ($n=3-6$) were vapor deposited onto the Ag(111) surface. The adsorption and structural ordering was investigated by thermal desorption spectroscopy, low-energy electron diffraction, and scanning tunneling microscopy. For all molecules we observe highly ordered monolayers with flat-lying molecules and long-range ordered domains of several hundred Å diameter. For the two smaller oligomers (EC3T and EC4T), two phases—a commensurate (relaxed) and an incommensurate (compressed)—are found, whereas the two longer molecules (EC5T and EC6T) form only incommensurate phases. The six unit cells exhibit significantly different symmetries, containing 1, 2, or 4 molecules. The formation of the geometric structures is discussed under the aspect of molecular size, molecular symmetry, and interplay of the molecule-substrate and molecule-molecule interactions. The last aspect was also investigated by concomitant force-field calculations. [S0163-1829(98)02143-2]

I. INTRODUCTION

Today the formation of long-range ordered superstructures of atoms or smaller molecules on crystalline metal surfaces is rather well understood from fundamental structural and energetic viewpoints.[1,2] This is, however, much less the case for larger organic molecules (typically with masses far above 100 amu) with sizes that are large with respect to the unit mesh of metal surfaces. It was even anticipated that such large organic molecules would not form ordered superstructures due to a likely dissociation, a lack of surface mobility, or a high configurational entropy. Of course this is not true, because a number of well-ordered systems with large organic molecules on different metal surfaces were reported in the past.[3–7] Therefore, two main questions can be put forward: (i) under what conditions do organic molecules form long-range ordered structures on metal surfaces, and is there an upper limit for the molecular size, and (ii) can these structures be understood or even predicted from energetic and/or kinetic viewpoints?

We emphasize that we consider metal surfaces here because these may provide considerable covalent interaction with the molecule, and the lateral ordering at least in the monolayer will be a consequence of the interplay of both the substrate-adsorbate *and* the adsorbate-adsorbate interactions. As one of the most obvious consequences, organic monolayers with superstructures that are *commensurate* to the substrate surface can be induced in this case.[5] This situation is significantly different from the one that is found on inert substrates, e.g., graphite or metal chalcogenides, on which *incommensurate* superstructures preferentially form due to the only weak-molecule surface bonding.[8–12]

The aim of this investigation was to obtain information on the above described aspects by a systematic comparison of the geometric ordering of chemically similar, but geometrically different molecules on the same surface. For this purpose we have used a particular series of oligothiophenes with different chain lengths, $n=3-6$ (see Fig. 1), which were vapor deposited onto an Ag(111) surface. These molecules are denoted as *end-capped* oligothiophenes (ECnT), because their terminal positions are blocked with cyclohexene rings (*end caps*) in order to increase their chemical stability.[13] Due to the variation of the molecular length (19.1–30.6 Å) and symmetry [C_i, C_S, or C_2 (Ref. 14)], different ordering behaviors and superstructures can be expected. Nevertheless, a comparison of these aspects for the different oligomers is reasonable, since all molecules exhibit the same, or at least a

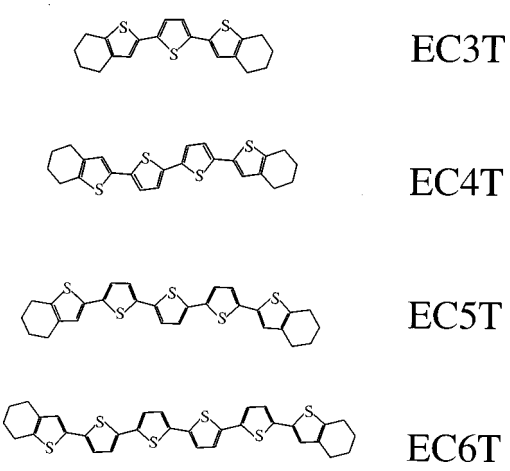

FIG. 1. Structure of the end-capped oligothiophenes (EC3T–EC7T). Note that the end caps (cyclohexene rings) are not planar due to sp^3-hybridized C atoms. Consequently, the molecules strictly exhibit only C_2, C_S, and C_i symmetry instead of C_{2v} and C_{2h}, depending on the relative conformation of the cyclohexene rings (see also Ref. 14).

very similar, chemical bonding to the surface via the π system.[6,15,16]

In order to obtain more quantitative information about the relevant interactions, we have also performed molecular modeling calculations in addition to the experiments. These were carried out for monolayers of EC4T, which we consider as somehow representative. These calculations take into account the van der Waals and electrostatic interactions. Hence, the obtained total packing energies contain neither the covalent bonding forces between molecules and the surface nor the surface-mediated intermolecular forces. From a comparison of experimental and computational results, it is thus possible to draw indirect conclusions on the relevance and size of the covalent forces.

We note that oligothiophenes are of technological interest, too, because films of this material class are presently investigated under the aspect of possible applications, e.g., in field-effect transistors[17] or light-emitting devices.[18,19] Since the device characteristics are also strongly determined by structural defects in the film and at the contact interfaces, the growth of high-quality epitaxial oligothiophene films on crystalline substrates is an attractive aim. For instance, a significant improvement of luminescence yields could be achieved for *epitaxial* quaterthiophene films with respect to films deposited on glass.[20–22] It is evident that a detailed understanding and probably a control of the adsorption geometry of the monolayer is decisive for the optimization of epitaxial growth of organic materials.

Ordered monolayers of different oligothiophenes were reported for various surfaces of noble metals (Ag, Au). The use of these surfaces appears to be a key to achieving high structural order, because on these surfaces no molecular dissociation occurs and the bonded molecules still exhibit sufficient lateral mobility for two-dimensional (2D) ordering. For the *unsubstituted* oligothiophenes (αnT) structures of α2T (Ref. 23) and α4T (Ref. 15) on Ag(111) and of α6T on Au(110) (Ref. 24) were observed. Results for EC4T and EC5T monolayers on Ag(111) were partially described in Refs. 6 and 25. In all cases the molecules adsorb in a coplanar (''flat'') geometry on these surfaces, which is caused by a preferential bonding to the metal surface via the conjugated π system.[5,15] In the case of EC2T,[26] EC4T,[27] EC6T,[27] and α4T,[15] this adsorption geometry was also clearly identified from the dichroism in near-edge x-ray absorption spectroscopy (NEXAS). Moreover, from the presence of differential chemical shifts in valence band ultraviolet photoemission spectroscopy (UPS) and NEXAS spectra it is consistently derived that the bonding of the molecules to the Ag(111) surface exhibits a *covalent* (chemisorptive) character.[5,15,28] Hereby we observe the trend of stronger differential shifts for the smaller molecules, indicating stronger surface molecule interactions. Further details of the electronic structures will be reported elsewhere.[28] Because of the covalent character of the substrate-molecule interaction it can be already expected (and is confirmed by our results) that the bonding is site specific, at least to some extent. In other words, one expects energetically preferred adsorption sites on the surface. This aspect is, of course, a very crucial point for the understanding of the formed structures, especially when commensurate and incommensurate structures are energetically compared, or phase transitions between these are considered.

This paper is organized as follows. Section II contains the experimental details. The data evaluation and the computational techniques used for molecular-modeling simulations are described in Sec. III. The experimental results are presented in Sec. IV, and a comparative discussion of the observed structures and the involved interactions is given in Sec. V. Summarizing conclusions are drawn in Sec. VI.

II. EXPERIMENTAL DETAILS

The experiments were performed in a multichamber UHV system with a base pressure of $\approx 10^{-10}$ mbar (for details see Ref. 6). The (111) surface of the silver single crystal was prepared by subsequent sputtering and annealing cycles at 700 K until x-ray photoemission spectroscopy (XPS) revealed a clean surface, and large defect-free terraces ($\geqslant$300 Å) were observed with low-energy electron diffraction (LEED) and scanning-tunneling microscopy (STM).

The synthesis of the ECnT molecules was described in Ref. 13. All materials were purified by several sublimation and recrystallization cycles before they were loaded into small glass crucibles of homemade Knudsen cells for vapor deposition onto the Ag(111) surface. In addition, the purity of the sublimated material was routinely controlled by taking mass spectra of the molecular beam using a Balzers QMG 511 quadrupole mass spectrometer (QMS). Typical temperatures of the crucibles during sublimation of EC3T, EC4T, EC5T, and EC6T were 110, 145, 190, and 255 °C, respectively. These allowed growth rates of about 0.5 monolayers/min (as calibrated by thermal-desorption spectroscopy). During deposition the Ag sample was held at $T_S = 200$–230 K for EC3T, EC4T, and EC5T, and at 300 K for EC6T. In the case of EC3T and EC5T systematic variations of T_S (135–300 K) and deposition rates (only EC3T) did not lead to different film qualities as judged, e.g., from the thermal desorption spectra (see Sec. IV A). In the case of EC4T, however, preparation at room temperature yielded thermal-desorption spectra with less sharp structures, indicating a less well-defined multilayer growth at elevated temperatures, probably caused by a nucleation of 3D microcrystallites due to higher surface mobilities of the adsorbing molecules (see also Ref. 6).

The temperature of the crystal was measured by a Chromel/Alumel couple that was fixed to the tantalum foil holding the crystal, because direct spot welding of the thermocouple onto the Ag crystal was impossible. For the temperature-scale calibration, see Ref. 6. For temperature programmed desorption (TPD) measurements [also known as thermal desorption spectroscopy (TDS)] typical heating rates of 0.5 K s^{-1} were used. Since experiments showed that the monolayers of all molecules do not desorb, the substrate was sputtered and annealed after each desorption experiment in order to obtain a clean surface (see also below). LEED investigations were performed with a three-grid LEED optics (Fisons Instruments/VG) with normal incidence of the electron beam onto the sample. The patterns were recorded with a reflex camera using high-speed films. Typical electron-beam energies were between 8 and 25 eV. The STM measurements were performed using a beetle-type STM (Ref.

29) in constant current mode with mostly positive tip voltages (U_t), utilizing and Ir/Pt tip. The here-shown STM images shown here were recorded using a $1/f$ highpass filter.

III. DATA EVALUATION AND COMPUTATIONAL METHODS

A. Evaluation of LEED and STM data

All geometric structures of the ordered monolayers were determined from the combination of LEED and STM data. The analysis involved three steps. First, the 2D mesh and the 2D space group of the superstructure was determined from LEED and STM data. Second, the orientation of the molecules within the unit cell was derived from STM images. In the third step, real-space models of the structures were developed, and the orientations of the molecules within the unit cells were refined such that the mutual overlap of the molecules was minimized. Hereby, we assumed that the π systems of the molecules (i.e., the conjugated thiophene rings) are fully planar and coplanar to the substrate, which is experimentally justified by the NEXAS data.[27] The nonplanar terminal cyclohexene rings (end caps) hence were assumed to be coplanar to the surface. However, a small tilt of the end caps with respect to the surface of the order of 30° cannot be excluded from the NEXAS and the here-reported STM data. The so-obtained geometric models describe the structures of the monolayers completely, except for the adsorption site (i.e., the relative position of the molecules with respect to the underlying substrate), which cannot be derived from such experiments.

The LEED patterns were evaluated by systematically fitting 2D reciprocal nets to the observed spot positions. Due to the smaller symmetry of the unit cells of the adsorbates with respect to the symmetry of the substrate there generally exist six symmetry-equivalent adsorbate domains on Ag(111). This was taken into account by incoherent superposition of the respective reciprocal nets. Special consideration was given to reproduce the azimuthal angles between the LEED spots, since these are insensitive to possible distortions of the patterns by small misalignments of the samples with respect to the center of the LEED optics. Due to the large number of spots in the diffraction patterns (e.g., see Fig. 3, below) the superstructures are unambiguously determined by this procedure. Hence, the numbers of the superstructure matrices exhibit a relative accuracy of about $\pm 1\%$. The absolute accuracy of the lattice constants determined by LEED is slightly smaller ($\pm 5\%$) due to the additional uncertainty of the absolute electron energy. Further details are described in Ref. 6.

The intensities of the LEED spots were not evaluated. However, the patterns were carefully examined at different electron energies to detect systematic absences of spots. These were used to determine the 2D space groups. We note that for the incommensurate superstructures the here-evaluated space groups refer only to the free-floating monolayers of the adsorbate, since there is no defined adsorbate-substrate registry in this case. For the commensurate and incommensurate phase of EC3T and the incommensurate phase of EC5T (see below), we observed systematic absences of LEED spots due to the existence of *glide lines* in the adsorbate layer, e.g., the absence of the $(H,0)$ spots for $H=2n$. These glide lines, however, do not constitute glide lines of the substrate. Therefore, multiple scattering effects and a small modulation of the adsorbate geometry due to the different adsorption sites could, in principle, lead to a small intensity contribution at the position of the above-mentioned spots. The fact that this was not observed indicates that the specific sites of the molecule on the surface have only a minor influence on the scattering here. This is probably due to the large size of the molecules, which somehow ''averages'' over many substrate atoms. (An example of a large molecule for which the $H=2n$ spots are observed was given in Ref. 30).

The lateral distances in STM images were calibrated by using a WSe_2 substrate. The absolute accuracy of the lattice constants of the molecular superstructures determined from STM images is about 1% and, thus, slightly higher than that of the LEED evaluation. Consequently, the given lattice parameters were predominantly derived from the STM data. Numerical 2D Fourier transformations of the STM images were found to be in good agreement with LEED results.

B. Computational methods

Geometric structures of the molecules that were used for the above structure determinations were obtained from force-field calculations[31] and were additionally verified by semiempirical quantum-mechanical calculations and [modified neglect of differential overlap (MNDO), Austin Model 1 (AM1)] using the parametrization PM3 (Ref. 32). The van der Waals radii were taken from Ref. 33. The molecular modeling calculations of the superstructures of EC4T were performed with the commercial program CERIUS^2 (Ref. 34) which was run on a Silicon Graphics workstation. In this case the geometric structure of the single EC4T molecule including partial charges was also determined by semiempirical quantum-mechanical calculations (MNDO) (Ref. 32), assuming C_i symmetry and a planar geometry of the π system. The parameters of the universal force field used in the molecular packing calculations were taken from Rappé, Colwell, and Casewit.[35] Two types of calculations of the total packing energy (TPE) were performed. First, the TPE was calculated for a free-floating 2D EC4T layer consisting of 3×3 unit cells with fixed lattice constants taken from the experiment. In these calculations the azimuthal orientation of the molecules within the unit cell was varied. Second, the TPE was calculated for this EC4T layer with a fixed geometry put onto the Ag(111) surface for different lateral and azimuthal positions, assuming an unreconstructed Ag(111) surface. As mentioned earlier, the TPE only includes Coulomb and van der Waals interactions, but not the covalent bonding forces between the molecules and the substrate and no-polarization effects between molecules.

IV. RESULTS

A. TPD characterization and monolayer preparation

In a first-step, multilayer films were characterized using TPD. Figure 2 displays a typical series of TPD spectra for different initial coverages of all four molecules. Two peaks labeled as α and β in Fig. 2 can be distinguished in all four series. In addition, a small and very sharp peak (γ) is observed for the two smaller members of the series EC3T and

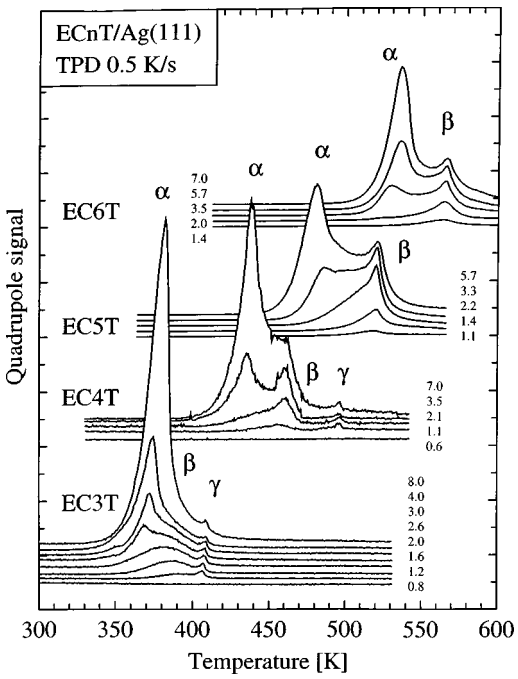

FIG. 2. TPD spectra for ECnT ($n=3-6$) molecules adsorbed on a Ag(111) surface. The various curves for each molecule belong to different initial coverages ranging from submonolayer to multilayers (7–8 ML). Masses of the intact ECnT molecules were monitored. The observed peaks are attributed to the multilayer (α, lowest temperature), the second layer (β peak, dominant for medium coverage), and a 7–9 % fraction of the monolayer (γ peak at highest temperature, only for EC3T and EC4T). The calibrated coverages are given in the figure in terms of monolayers of flat-lying molecules.

EC4T, at higher temperatures. From the combination of LEED, STM, XPS, NEXAS, and TPD measurements we find that the monolayer, i.e., the layer of flat-lying molecules that are directly bound to the substrate, cannot be thermally desorbed. Only in the cases of EC3T and EC4T can a small fraction of molecules be desorbed from the compressed first layer on the Ag surface leading to the sharp γ peak. The coverages of molecules that remain on the surface after heating just above the TPD peaks are referred to as *one monolayer* (ML) in the following. The initial coverages given in Fig. 2 were determined from the integrated TPD signals and calibrated to the corresponding number of ML by XPS and LEED.

The α peaks in Fig. 2 appear after higher exposure and cannot be saturated, and their maxima shift to higher temperatures with increasing initial coverage. This behavior is typical for the desorption of multilayers, and, therefore, we assign the α peaks to *multilayer desorption*. In contrast, the β peaks can be clearly saturated. Since the monolayers cannot be desorbed, the β peaks are thus attributed to desorption from the *second layer*. The β peaks are shifted to higher temperatures with respect to the α peaks (about 20–40 K). We explain this by a slightly larger binding energy of the molecules in the second layer compared to the binding energy of the higher layers. The likely reason for this is that the intermolecular forces between the second layer and the monolayer are indirectly modified due to the covalent bonding of the latter molecules to the Ag surface. The bonding modifies, e.g., polarizes, the valence orbitals, which are also responsible for the intermolecular interactions. From Fig. 2 we further derive that the α peaks appear for increasing initial coverage after the β peaks have approximately been saturated. From this and from concomitant LEED measurements we conclude that the films grow in an approximate layer-by-layer mode, at last for the first three layers, although conclusions from TPD concerning the film morphology and film growth have to be considered with caution.

It is interesting to note that in the case of EC4T the β peak is well separated from the dominant α peak only for a certain (optimum) range of preparation conditions, especially substrate temperatures.[36] Otherwise, it is smeared out and is only discernible as a shoulder of the α peak.[6] As noted above, this could indicate that the second layer is less well defined in case of not optimal preparation conditions. The shape of the β peak also varies for the investigated molecules. Whereas in the case of EC3T the peak is rather broad, and a small shift of the maximum to lower teperatures with increasing initial coverage can be seen, a much narrower peak and a constant maximum temperature are observed for EC4T, EC5T, and EC6T. Again, we interpret this as a reduced structural order and/or morphological quality of the second layer in the case of EC3T.

The peak γ is only observed for EC3T and EC4T. Its width is considerably smaller than that of the other peaks. The peak areas are about 8% of a ML for EC3T and EC4T and the peak positions are at 407 and 497 K, respectively. For both molecules the peak stems from the desorption of a small fraction of molecules from the first layer, which occurs when the ML undergoes a phase transition from a compressed (incommensurate) to a relaxed (commensurate) superstructure, which contains about 8% less molecules (see Sec. IV C). These structural phase transitions are also observed as changes in the LEED patterns. The desorption occurs in a likewise ''autocatalytic'' manner, since the desorption is driven by a considerable gain of energy due to the release of lateral compressive strain and the shift of the remaining molecules to energetically more favorable adsorption sites (see Sec. IV D). We also note that these phase transitions are reversible, which means that the peak γ can be reproduced by a subsequent small deposition of molecules onto the relaxed monolayers.

On the basis of the TPD results monolayers for structural investigations were prepared by adsorbing about 2 ML and by thermal desorption of the second layer. In order to avoid thermal decomposition of the molecules the temperature was increased only up to the falling high-temperature edge of the β peak. In the case of EC3T and EC4T, also two different procedures were used: Relaxed monolayers were prepared by annealing at 420 K (EC3T) and 520 K (EC4T), i.e., above the respective temperatures of the phase transitions (the γ peaks). Compressed monolayers were prepared by exposure of an initial coverage of about 1.2 ML and subsequent careful desorption at temperatures below the γ peak with concomitant LEED control.

B. Long-range order, domain formation, and submolecular STM contrast

After the application of the above preparation routine we systematically observed by LEED and STM that long-range

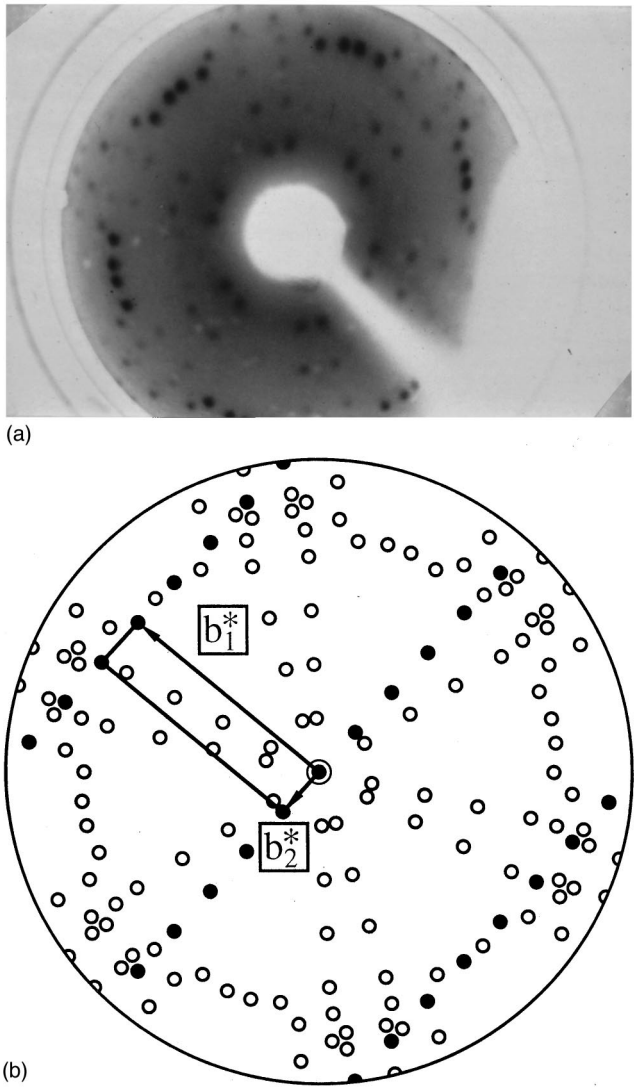

FIG. 3. (a) LEED pattern of a EC6T monolayer on Ag(111) taken at an electron energy of 11 eV. (b): Simulated LEED pattern with reciprocal unit vectors ($\mathbf{b}_1^*$,$\mathbf{b}_2^*$) as indicated. One of the six symmetry-equivalent domains is accentuated by full symbols. The 12 prominent radial spot rows stem from the (0,H) spots.

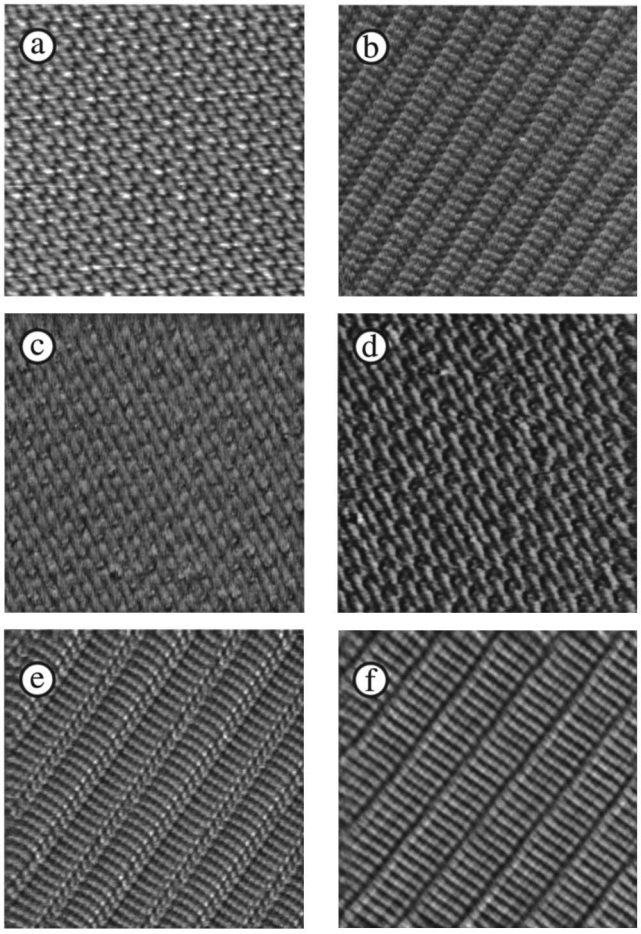

FIG. 4. Overview of STM images of the different ordered monolayers of end-capped oligothiophenes on Ag(111): (a) EC3T commensurate (*relaxed*) monolayer, (b) EC3T incommensurate (*compressed*) monolayer, (c) EC4T commensurate (*relaxed*) monolayer, (d) EC4T incommensurate (*compressed*) monolayer, (e) EC5T incommensurate monolayer, (f) EC6T incommensurate monolayer (scan sizes: 174 Å$\times$174 Å). Note than in the case of EC4T (c) and (d), the STM images represent reflectional domains of the structures shown in Figs. 6(c) and 6(d).

ordered superstructures had formed. This result applies to all four oligothiophenes. Sometimes the LEED superstructure patterns were not optimal (sharp spots, low background) directly after the initial preparation; but in this case we were able to improve their quality by additional short annealing cycles. From the STM images we derived that monolayers prepared in this way exhibit ordered domains of a size of several hundred Å in diameter (about 400–1000 Å). This is consistent with the observation of sharp LEED superstructure spots, which were limited only by the instrumental transfer width of about 150 Å. An example for such a LEED pattern is shown in Fig. 3(a) for EC6T on Ag(111). LEED patterns of equal qualities were obtained for all six structural phases (see below), which are formed by the four different molecules. (LEED patterns of EC4T and EC5T were reported in Refs. 6 and 25.)

The high-quality two-dimensional ordering was also derived by STM. Figure 4 gives an overview of STM scans of all structures. The molecules are imaged as elongated objects, and evidently all molecules lie flat on the surface. Notably point defects due to impurities, missing, or mispositioned molecules or molecules with a different structural conformation within the domains were found very rarely. From STM images we derived that the domains were limited either by structural imperfections of the substrate, e.g., steps, or by domain boundaries between different symmetry-equivalent domains. However, we could never observe phase boundaries between translationally equivalent domains (see also Ref. 6), which indicates that the molecules are highly mobile on the Ag(111) surface during the annealing cycles used for the monolayer preparation. For EC4T a high-surface mobility can be also deduced for room temperature, because for this molecule, ordered monolayers were also prepared without additional annealing. We note that we observed a high mobility on the Ag(111) surface for many other large organic molecules at room temperature,[5,7,30] which reveals that the lateral corrugation of the molecule-surface bonding potential is only small.

In the STM images (Fig. 4) the molecules are imaged as either straight EC4T and EC6T or curved (EC3T and EC5T) elongated objects, as expected from the form of the all-transconformations shown in Fig. 1. It is also interesting to make a few brief comments on the intramolecular STM contrasts at this point. Two different types of images of the single molecules can be distinguished. In the first case the molecules are imaged as rather compact objects without any internal structure. This case is found for both phases of EC4T [Figs. 4(c) and 4(d)] and the commensurate phase of EC3T [Fig. 4(a)]. Especially for EC4T the bonelike overall shape of the molecule, which is due to the nonplanar and slightly more spacy end caps (see also Fig. 1), is well reproduced in the STM images. In the alternative case the molecules show a strong submolecular structure containing distinct maxima. This type of submolecular STM contrast was observed for the incommensurate phase of EC3T [Fig. 4(b)] and for the ordered monolayers of EC5T [Fig. 4(e)] and EC6T [Fig. 4(f)]. The number of observed maxima corresponds to the number of the thiophene units plus two. Thus, we assign these maxima to the thiophene units and the two cyclohexene end caps of each molecule. This assignment is also corroborated by STM images of ordered layers with point defects due to mispositioned molecules.

We can only speculate about the reason for these two types of STM contrasts at present. It is, however, remarkable that the STM contrast and the geometric structures of the phases appear to be correlated: in the first case the molecules are arranged in a *brick-wall-like* structure, whereas in the second case the molecules form parallel *stacks*. One reason may be that the second type of lateral packing leads to a very subtle change of the electronic and/or geometric configuration of the molecules with respect to those in the former packing. For example, the thiophene rings and the end caps may be slightly twisted with respect to the surface (by some degrees). Due to the nonlinear character of the tunnel junction the STM contrast is extremely sensitive to such small modifications of the molecules, which may cause the observed difference in the STM contrast, possibly in combination with a specific conformation of the STM tip. (For a further discussion, see also Ref. 25.)

Finally, we note that during the STM investigations we found, of course, also disordered regions between long-range ordered domains due to a not optimal layer preparation or surface imperfections, e.g., steps. Figures 5(a) and 5(b) display two examples of wide-area STM images of EC4T and EC6T monolayers. These images are untypical in so far as they were deliberately taken from surface regions with imperfect lateral order. The area shown in Fig. 5(a) is nearly covered by a single-ordered domain. In the upper right part of the image there is a monoatomic step, and in the vicinity of this step one can observe small disordered regions or individual molecules that appear to be structurally modified, e.g., bent. It is further notable that the lateral order is not significantly distorted by the step that evolves from the screw dislocation at the left side of Fig. 5(a) or by the ''contamination'' in the left bottom region. These observations indicate that the lateral order of the EC4T molecules must be rather robust. Figure 5(b) is interesting in a different way: it shows a region of an EC6T monolayer in which strong disorder is to be seen. Two ordered domains, which are rotated by 120° with respect to each other, can be recognized in the upper left corner and on the bottom. Between these domains there is a disordered, fluidlike phase that, nevertheless, exhibits some short-range order, since plenty of small ordered clusters with a size of about 3–10 molecules can be distinguished in this phase.

C. Geometric structures

We now turn to the geometric structures of the observed phases. The parameters of all structures are listed in Table I. Since EC3T and EC4T both yield a compressed as well as a relaxed phase, there exist all in all six different structures, which are summarized in Table I. Figure 4 shows the corresponding STM images; the corresponding real-space models are given in Fig. 6.

On our data we make the following observations.

(1) In all cases the molecules are adsorbed with their molecular planes parallel to the surface, as derived from NEXAS (Refs. 15 and 27), in agreement with the STM images (Fig. 4). This is understandable from the presence of the covalent bonding to the surface via the π system.[15,5] From the STM images and from the space requirements of the molecules in real-space models we conclude further that all four oligomers are in an all-transconformation on the surface, as shown in Figs. 1 and 6. The concentration of molecules that are not in all-transconformation must be very small, since we expect such molecules to distort the geometric order at least locally due to their different shape in a similar manner as point defects, e.g., due to impurities. This result is not trivial, since we found by semiempirical quantum–mechanical calculations (AM1) for the free oligomers that the all-transconformations of the thiophene units have the smallest energies, but that the energy difference to non-all-transconfigurations is only small, i.e., that the energy of a cisconformation of two thiophene rings is only about 5 kJ mol^{-1} larger than that of the transconformation.

(2) From the real-space models of Fig. 6 it is obvious that a close packing of the molecules is achieved in all incommensurate phases. The close-packed structures maximize the energy gain from the attractive molecule-surface bonding, which thus appears to be a general and important principle for the lateral ordering.

(3) Two different types of structures are observed. In the compressed phase of EC3T [Fig. 6(b)] and in the structures of EC5T [Fig. 6(e)] and EC6T [Fig. 6(f)], the molecules are ordered in parallel stacks (2D *stacking* structures), whereas *brick-wall-like* structures are observed for the relaxed phase of EC3T [Fig. 6(a)] and both phases of EC4T [Fig. 6(c) and 6(d)].

(4) For the molecules with an *even* number of thiophene rings the unit cell contains *one* molecule. For those with an *odd* number of rings, unit cells with 2 or 4 molecules are found. The spacegroup is $p211$ for the primitive unit cells,[37] whereas it is $p2gg$ or $p1g1$ for the unit cells containing more than one molecule (see Table I). The latter space groups contain additional glide planes (see Fig. 6), which result in systematic absences of spots in the corresponding LEED patterns, as observed. For the molecules investigated here, there thus exists a correlation of the space group and the symmetry of the molecule. The reason for this behavior is not quite clear. A possible reason was derived from semi-

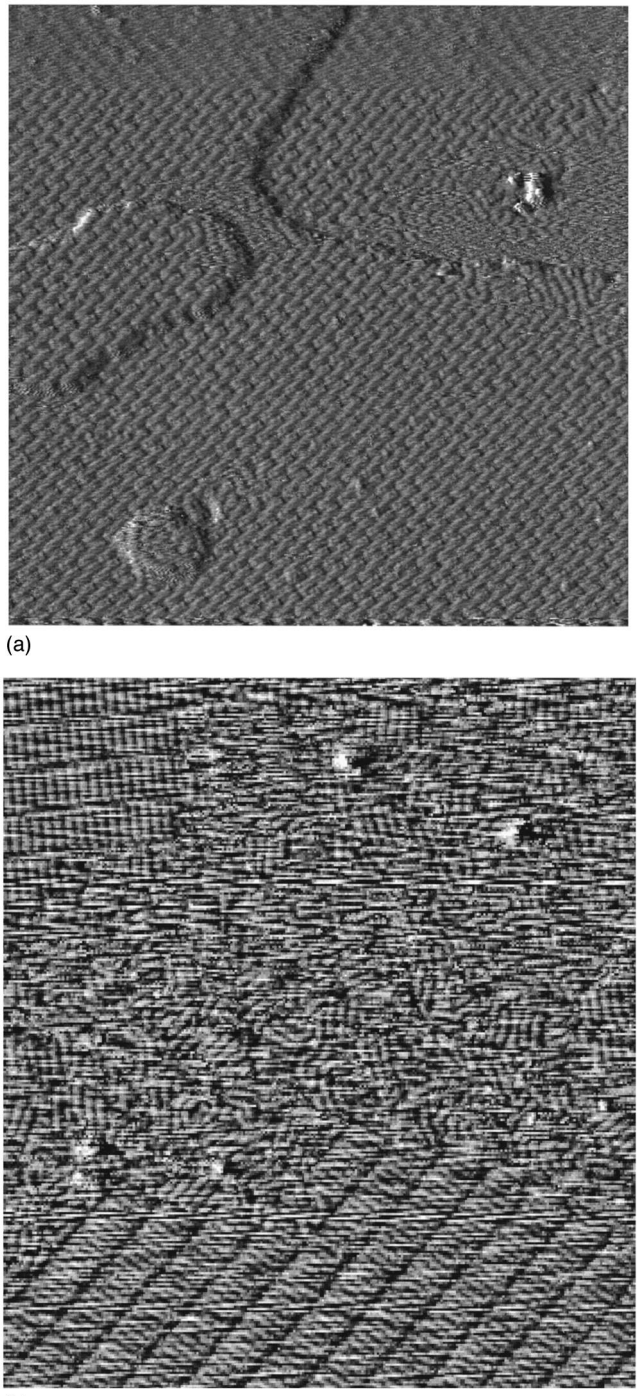

(a)

(b)

FIG. 5. (a) Large area STM scan of an EC4T monolayer on Ag(111) (incommensurate phase). This image was deliberately taken from an area where the Ag(111) surface exhibits several defects in order to illustrate their influence on the order of the organic monolayer. A screw dislocation is visible on the left-hand side, a monoatomic step can be seen in the upper right corner and a small protrusion, probably due to surface contaminations, is found in the left bottom corner (scan size: 352 Å×352 Å, $U_t = 2.6$ V, $I = 0.7$ nA). (b) Large area STM scan of an EC6T monolayer on Ag(111). The image was taken from an area, where considerable disorder is observed. Note the two ordered regions, which belong to two different 120° rotational domains, at the upper left corner and at the bottom (scan size: 425 Å×480 Å, $U_t = 1.6$ V, $I = 1.2$ nA).

empirical quantum-mechanical calculations (MNDO and AM1), which showed that the odd-numbered molecules exhibit a small electric-dipole moment.[38] This would make an antiferroelectric ordering of the stacks more favorable, as observed here (see Fig. 6).

(5) All three *stacking structures* [Figs. 6(b), 6(e), and 6(f)] are very similar due to the following facts: First, all these structures exhibit a nearly rectangular unit cell and the same vector $\mathbf{b}_1$ as the shorter vector of the superstructure unit cell. Second, the long axes of the molecules are parallel (EC3T, EC5T)—or at least nearly parallel (EC6T)—to the longer unit cell vectors $\mathbf{b}_2$. The constant length of $\mathbf{b}_1$ can be understood because this vector is about perpendicular to the long axis of the molecules, and its length is thus related to the constant width of the molecules (see Fig. 6). As a consequence of the identical directions of $\mathbf{b}_1$ with respect to the substrate, the orientation of the molecular stacks with respect to the substrate is also the same in all three structures.

(6) It is remarkable for the two shorter molecules (EC3T and EC4T) that *commensurate* superstructures are observed in addition to the *incommensurate* (compressed) structures. (In Table I the commensurate superstructures are identified from superstructure matrices with integer numbers or half integer numbers, whereas the incommensurate structures have noninteger matrix elements.) The differences in coverage (9% and 7%, respectively) between the commensurate and incommensurate structures (calculated from the two structure models) correspond well to the observed areas of the above-discussed desorption peaks γ (Sec. IV A). The main difference between the commensurate and incommensurate structures is that in the commensurate structures each unit cell (or at least every second unit cell, as in the case of EC3T) exhibits the identical position with respect to the substrate surface, whereas the relative position with respect to the substrate varies from unit cell to unit cell for the incommensurate structures. As a consequence there exists one distinct and energetically preferred adsorption site in the commensurate structure of EC4T. In the case of EC3T the situation is slightly more complicated, since the unit cell contains four molecules and the structure is commensurate only in *higher order* (here, ''second order''). Thus, there are eight different adsorption sites in this structure. However, the formation of commensurate structures demonstrates the influence of the substrate surface on the lateral ordering of both molecules.

(7) The incommensurate and commensurate phases of EC3T could be well distinguished in STM images, since the two structures are significantly different [see Figs. 4(a) and 4(b)], and a large number of STM images of both structures could be recorded. Quite differently, we obtained only very few STM images in which we could identify the incommensurate phase of EC4T [see Figs. 4(d) and 5(a)], albeit we investigated many samples that showed the LEED pattern of the incommensurate EC4T phase prior to the STM investigations. One possible interpretation for this observation would be a tip-induced phase transition of the incommensurate to the commensurate phase that is initiated by the interaction between the STM tip and sample and/or the electric field of the tip.

TABLE I. Comparison of monolayer structures of the investigated end-capped oligothiophenes on Ag(111) (EC3T–EC6T). The top row of the superstructure matrix is $\mathbf{b}_1$, the bottom row $\mathbf{b}_2$, in units of the substrate unit cell vectors $(\mathbf{a}_1,\mathbf{a}_2)$ (cf. Fig. 6). $\mathbf{b}_1$, $\mathbf{b}_2$ denote the unit vectors of the superstructure cell (see Fig. 7, below), γ the included angle, Φ the angle included by $\mathbf{b}_1$ (the shorter unit cell vector) and the [101] direction of the Ag(111) surface $(\mathbf{a}_1)$, i.e., the direction of the close-packed Ag rows.

Molecule	Superstructure matrix[1]	Number of molecules per unit cell	Space group	Geometric parameters	Comment
	$\begin{pmatrix} -4 & -8 \\ 8.5 & 0 \end{pmatrix}$	4	*p2gg*	$\mathbf{b}_1 = 20.0$ Å $\mathbf{b}_2 = 24.6$ Å $\gamma = 90.0°$ $\Phi = -90.0°$	relaxed layer; commensurate in second order [Fig. 6(a)]
EC3T					
	$\begin{pmatrix} 2.6 & 1.0 \\ 1.7 & 12.8 \end{pmatrix}$	2	*p1g1*	$\mathbf{b}_1 = 6.6$ Å $\mathbf{b}_2 = 34.8$ Å $\gamma = 90.6°$ $\Phi = 22.4°$	compressed layer; incommensurate *stacking structure* [Fig. 6(b)]
	$\begin{pmatrix} -3 & -5 \\ 5 & 1 \end{pmatrix}$	1	*p211*	$\mathbf{b}_1 = 12.6$ Å $\mathbf{b}_2 = 13.2$ Å $\gamma = 107.4°$ $\Phi = -83.4°$	relaxed layer; commensurate [Fig. 6(c)]
EC4T					
	$\begin{pmatrix} -3 & -4.7 \\ 5 & 1 \end{pmatrix}$[a]	1	*p211*	$\mathbf{b}_1 = 11.9$ Å $\mathbf{b}_2 = 13.2$ Å $\gamma = 110.1°$ $\Phi = -99.1°$	compressed layer; uniaxial incom mensurate [Fig. 6(d)]
EC5T	$\begin{pmatrix} 2.6 & 1.0 \\ 2.6 & 18.8 \end{pmatrix}$	2	*p1g1*	$\mathbf{b}_1 = 6.6$ Å $\mathbf{b}_2 = 51.3$ Å $\gamma = 90.2°$ $\Phi = 22.4°$	incommensurate *stacking structure* [Fig. 6(e)]
EC6T	$\begin{pmatrix} 2.6 & 1.0 \\ 1.9 & 10.8 \end{pmatrix}$	1	*p211*	$\mathbf{b}_1 = 6.6$ Å $\mathbf{b}_2 = 28.9$ Å $\gamma = 88.2°$ $\Phi = 22.4°$	incommensurate *stacking structure* [Fig. 6(f)]

[a]Corresponds to the matrices given in Ref. 6, which were set up for an angle between $\mathbf{a}_1$ and $\mathbf{a}_2$ of 60° instead of 120°.

D. Energetic considerations

A quantitative evaluation of TPD spectra principally allows us to determine activation energies for desorption of molecules from the film. This has successfully been done for many small molecules.[39] Among the important prerequisites are an accurate calibration of the temperature scale, a sufficiently well-determined background, and good signal-to-noise ratio. For the here-used mounting of the thermocouple (cf. Sec. II) and the here-investigated large molecules these requirements are hardly fulfilled, and there are additional sources for systematic errors. For example, errors may be caused by the fact that due to high sticking coefficients on all surfaces the QMS does not measure the partial pressure (as usual for small molecules), but the desorbing flux crossing the ionization volume of the QMS. In addition, the monitored flux may be modified by a varying angular distribution, and thus may be not proportional to the total desorption rate, which is required for the evaluation.[39]

Although being aware of these problems, we have evaluated the multilayer desorption peaks (α) in order to determine the activation energies (E_D) for multilayer desorption. For this purpose we used the leading-edge approximation.[40] The obtained E_D values are listed in Table II and may be subject to the above-mentioned systematic errors. However, we expect that the determined desorption energies are at least good estimates for the correct values and that trends of the values, e.g., as a function of the molecular size, are correctly reproduced. We find that E_D increases systematically from 140 to 230 kJ mol^{-1} from EC3T to EC6T, as it could be already expected from the systematic shift of the peak positions towards higher temperatures with increasing chain lengths (Fig. 2). Since the values of E_D are probably a good measure of the effective binding energies of the ECnT molecules in the film, they are also related to the intermolecular interactions. (This correlation is based on reasonable assumptions such as that the desorption kinetics are compa-

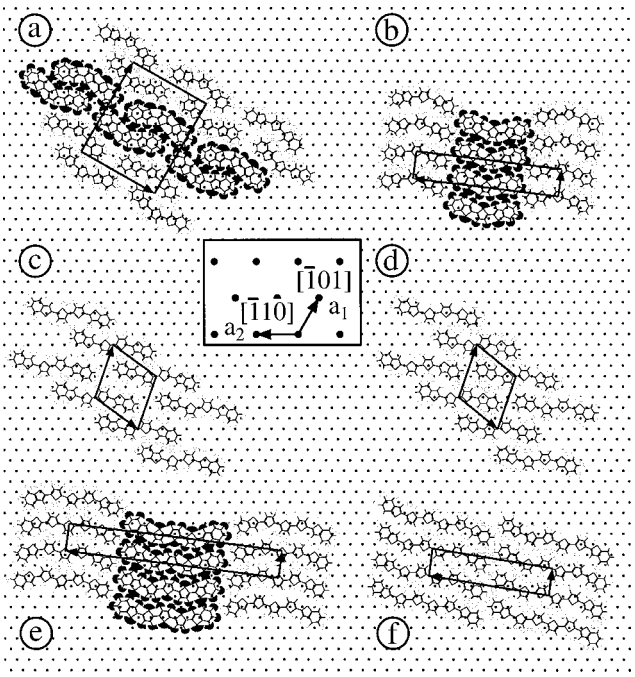

FIG. 6. Structure models (real space) of ordered monolayers of different end-capped oligothiophenes on Ag(111): (a) EC3T commensurate (*relaxed*) monolayer, (b) EC3T incommensurate (*compressed*) monolayer, (c) EC4T commensurate (*relaxed*) monolayer, (d) EC4T incommensurate (*compressed*) monolayer, (e) EC5T incommensurate monolayer, (f) EC6T incommensurate monolayer. The inset shows the substrate unit cell vectors. The van der Waals spheres of the atoms are partially indicated in order to illustrate the space requirement of the molecules.

rable in all systems and that there exist no significant energetic barriers in the desorption paths in front of the surface.) In the following we will thus use E_D as an estimate for the intermolecular interactions. We find E_D to scale very well with the mass of the molecules (within 5%), but somewhat less well with the number of π electrons. This may indicate that the π electrons (which are mainly localized on the thiophene rings) do not play a more dominant role than the cyclohexene end caps for the intermolecular interactions.

We now turn to the monolayers. Here the most important interaction is the covalent bonding of the π system to the Ag substrate, i.e., the adsorption energy (E_{sub}), which causes the flat adsorption geometry of the molecules. At least for the two shorter oligomers this bonding potential also has a significant corrugation parallel to the surface, which causes the site-specific adsorption in the commensurate phases of EC3T

TABLE II. Overview on energy parameters. T_α are the peak temperatures of the multilayer desorption peaks of Fig. 2, and E_D are the desorption energies. The error limits are (conservative) estimates for the *absolute* values.

Molecule	Mass (amu)	T_α (K)	E_D (kJ mol^{-1})
EC3T	356	382±8	140±30
EC4T	438	438±9	175±30
EC5T	520	481±10	215±30
EC6T	602	536±11	235±30

and EC4T (E_{sub} cannot be measured by TPD, since the molecules in the monolayer cannot be thermally desorbed from the surface, but dissociate upon annealing.) We note that calculations of this interaction are presently impossible, since the modeling of the covalent bonding requires *ab initio* calculations, which presently cannot handle adsorbate/substrate clusters of such large molecules.

However, it is at least, in principle, possible to estimate the size of E_{sub} from the intermolecular interactions and the formation of relaxed and compressed phases by EC3T and EC4T. The idea is that the energy gain due to adsorption of additional molecules (E_{sub}) into the relaxed (commensurate) phases must overcompensate the energy necessary to force the molecules out of the optimum adsorption sites plus the additional lateral compressive strain within the more compressed layers. Both energetic contributions are induced at the same time by the adsorption of additional molecules. We will at first give a general description of the energy balance for the example of EC4T and afterwards we will discuss some values relevant for EC4T in more detail. (However, an analogous discussion applies also to EC3T.)

When additional molecules are adsorbed into the relaxed monolayer, the surface energy is lowered by two contributions. First from the *molecule/substrate bonding*, and second from the *attractive lateral intermolecular interactions* to the additional molecules. We denote the average values per molecule as E_{sub} and E_{attr}.[41] Thus, the average energy per molecule that is gained when additional molecules are adsorbed into the relaxed monolayer ($\Theta = 0.93$ ML) up to a fully compressed monolayer ($\Theta = 1$ ML) is $(1-\Theta)(E_{\mathrm{sub}}+E_{\mathrm{attr}}) = 0.07(E_{\mathrm{sub}}+E_{\mathrm{attr}})$. This energy gain must be larger than the additional average compressive strain per molecule (E_{strain}) plus the average energy to force the molecules of the commensurate phase ($\Theta = 0.93$ ML) out of their optimum adsorption sites (ΔE_{sub}). This yields the condition: $0.07(E_{\mathrm{sub}} + E_{\mathrm{attr}}) \geq E_{\mathrm{strain}} + 0.93\Delta E_{\mathrm{sub}}$ which is equivalent to

$$0.07E_{\mathrm{sub}} - 0.93\Delta E_{\mathrm{sub}} \geq E_{\mathrm{strain}} - 0.07E_{\mathrm{attr}}. \qquad (1)$$

This equation compares the adsorbate/substrate interactions (on the left side) with the intermolecular interactions (on the right side).

It is, of course, difficult to estimate E_{sub} from Eq. (1), since the intermolecular interactions on the right side are also subject to the covalent bonding to the substrate, which causes the respective energies to differ from those expected within free-floating layers of the molecules and they are, thus, essentially unknown (see also below). Nevertheless, we can make some reasonable assumptions, which at least allow to estimate the relative orders of magnitude of the energy terms. First of all, we assume that ΔE_{sub} is much smaller than E_{sub} and set $\Delta E_{\mathrm{sub}} = 0$. This assumption is motivated since we observe a high-surface mobility, which points to an only small lateral corrugation of the bonding potential and, thus, a small value of ΔE_{sub}. As a consequence we obtain a lower estimate for E_{sub} from Eq. (1). In addition, we also neglect E_{attr}, since we expect this energy to be of the order of the intermolecular interactions, which were estimated by E_D (see above), and thus to be smaller than E_{sub} by about at least one order of magnitude.

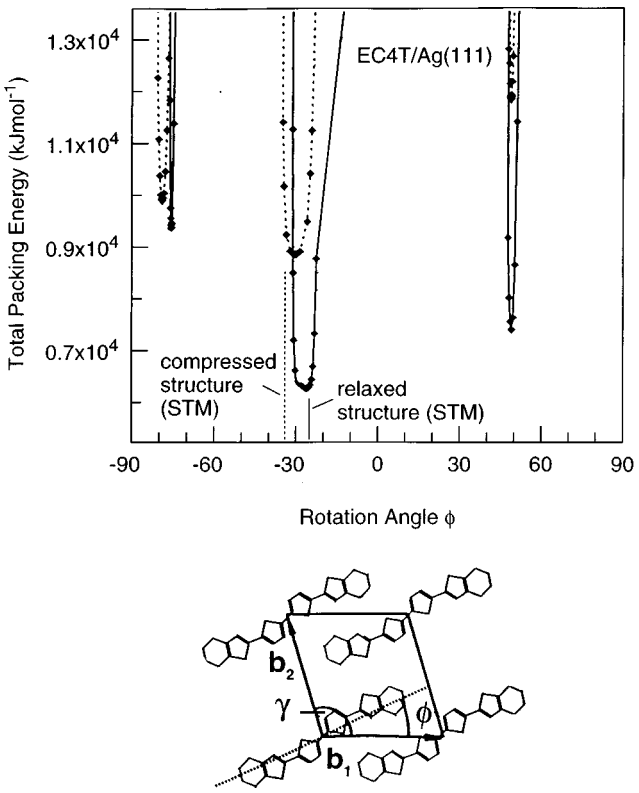

FIG. 7. Calculated total packing energies of free-floating EC4T layers containing 3×3 unit cells and using the experimentally determined parameters of relaxed (full curves) and compressed (dashed curves) superstructures. The angle ϕ that is included by the long axis of the molecule and unit cell vector $\mathbf{b}_1$ (see inset) was systematically varied. Note that for both structures the absolute energy minima coincide with the values of ϕ determined by STM (vertical lines).

Thus, the most relevant energy that has to be balanced by the molecule/substrate interaction (E_{sub}) is the energy due to the lateral compressive strain or, in other words, the lateral repulsion between the molecules (E_{strain}). In order to demonstrate the influence of the strain on the structures, we have performed molecular modeling calculations for a *free floating* EC4T layer consisting of 3×3 unit cells. Figure 7 shows as a result the TPE that were obtained for the compressed and relaxed phases of EC4T using the *experimentally* determined (and in the calculation fixed) dimensions of the unit cell. The only parameter that was varied in these calculations was the angle ϕ, which is defined as the angle included by the long axis of the molecule and the short axis $\mathbf{b}_1$ of the unit cell (see inset of Fig. 7).

We will first discuss Fig. 7 and consider its limitations, and will then turn back to the estimation of the adsorption energy. The following results are derived from Fig. 7. First, for both phases there exist three pronounced minima of the TPE as a function of ϕ. The small widths of the minima (5°–10°) indicate that the molecules are rather close packed to each other and that little space exists for a variation of their azimuthal positions in these structures. The position of the minima of the TPE differs only by a few degrees for the relaxed and compressed phases, which is understandable because both structures transform into each other by an only small change (6%) of the length of the unit cell vector $\mathbf{b}_1$ (cf. Table I). Second, the values of the TPE are large and positive. This indicates that the experimentally determined intermolecular distances are smaller than they would be on the basis of the pure intermolecular interactions, and that the intermolecular interactions of the free-floating layer are thus strongly repulsive at these small intermolecular distances. The repulsion comes from the overlap of the mutual wave functions of the terminal atoms (Pauli repulsion) and can also be envisaged from the small overlap of the van der Waals spheres in Figs. 6(c) and 6(d).[42]

Third, we find that the absolute minima of the TPE coincide well with the values of ϕ determined from STM images, which indicates that the geometric requirements are modeled correctly. The fourth result, which we obtain from Fig. 7, is that the TPE of the compressed 3×3 EC4T ensemble (dashed line in Fig. 7) is larger than the TPE of the relaxed EC4T 3×3 ensemble (continuous line) by a value of 2.500 kJ mol^{-1}. Thus, we would estimate the average compressive strain per molecule (E_{strain}) to be at least of the order of $\frac{1}{9}$ of this value (i.e., 280 kJ mol^{-1}), keeping in mind that we have used open boundaries that likely underestimates the TPE per molecule with respect to the TPE per molecule of an infinite layer. On the basis of this modeling calculation we thus derive that the incommensurate layer is indeed significantly strained with respect to the commensurate layer, which explains well why the desorption peak γ (see Fig. 2), which is related to the phase transition from the compressed to the relaxed monolayer, is so sharp. We note that such an overlap of the terminal van der Waals radii in a monolayer of an organic adsorbate was also identified as the reason for the significant band dispersion of valence orbitals, e.g., observed for benzene on Ni(111).[43]

Using this value of E_{strain} we estimate that E_{sub} is larger than 4000 kJ mol^{-1} from Eq. (1) ($E_{\text{sub}}\geq E_{\text{strain}}/0.07$). This value would indicate a very high adsorption energy even for such a large and chemisorbed molecule as EC4T. (For comparison, the bonding energy of one covalent sulfur-carbon bond is about 220 kJ mol^{-1}.) A large value of E_{sub} is, nevertheless, expected, because it explains (i) why the molecules cannot be thermally desorbed from the surface, and (ii) why a flat-lying bonding geometry is so strongly preferred on Ag(111) even for the longer chain ECnT's, whereas a tendency for adsorption of the unsubstituted oligothiophenes (e.g., α5T, α6T) in an upright geometry, which is driven by the intermolecular interactions, occurs on more inert substrates.[44]

The major contribution of the molecule/substrate interaction (E_{sub}) stems from the covalent part of the interaction; only a minor contribution is added by van der Waals and electrostatic interaction with the substrate. We derived this from the comparison of the TPE calculated for the free-floating relaxed EC4T 3×3 ensemble and the same ensemble brought into contact with an Ag(111) surface (with the intermolecular distances kept fixed). The lateral and azimuthal position of the EC4T ensemble with respect to the surface was optimized before the final TPE was determined. It is notable that this procedure also yielded the experimentally observed commensurate structure, which means that the correct azimuthal orientation was determined by the search for the minimum in the TPE. From comparison we found that the TPE is lowered by the attractive bonding to the

Ag(111) surface by about 750 kJ mol^{-1} (per molecule) with respect to the free-floating layer. Since this energy is considerably smaller than the above estimated value of E_{sub} and since the TPE calculations contain only the *noncovalent* interactions, we can conclude that the dominant part of the substrate interaction must indeed be due to covalent bonding forces.

However, we believe that the here-estimated value of E_{sub} is significantly overestimated because a too large energy of the lateral strain (E_{strain}) was obtained from our modeling calculation due to a systematic shortcoming of the here-performed modeling calculation for the (free-floating) monolayer. The plausible reason is that the lateral intermolecular interactions are also significantly modified by the covalent bonding of the molecules to the surface and are thus not correctly described in the molecular modeling calculation by the used force fields. Especially, the intermolecular forces are presumably not that strongly repulsive as it is suggested by the large value of E_{strain} derived from the calculations. One obvious reason for this is that the geometry of the molecules is slightly changed by the adsorption on the surface. This may include, e.g., (i) small distortions of the molecular backbone and (ii) an upwards bent of the terminal H atoms out of the molecular plane, as e.g., postulated for planar aromatic molecules on Pt(111).[45] We expect these effects to reduce the net lateral extension of the molecules, and thus to reduce the repulsive interactions. In addition, for a chemisorbed molecule like EC4T there may also exist a substrate mediated *attractive* component of the intermolecular interaction, as it was indirectly concluded, e.g., for 3,4,9,10-pesylenetetracarboxylic dianhydride (PTCDA) on Ag(110) which partially compensates the repulsive forces. As a consequence of such corrections, a lower value of E_{strain} and thus a lower value of E_{sub} would be derived by Eq. (1).

In conclusion, we found that molecular modeling calculations, which do not account for the covalent bonding to the surface, have to be considered with care for chemisorbed layers of organic molecules. However, two interesting results are, nevertheless, obtained for the case of EC4T Ag(111): (i) the molecular substrate interaction is large and leads to a lateral compression of the molecules and (ii) the intermolecular interactions within the monolayer appear to be modified with respect to those of free molecules, since otherwise an unphysically high lateral strain would result.

V. DISCUSSION

All molecules investigated here form long-range ordered monolayers on Ag(111), irrespective of the chain length. No indication for a considerable influence of entropy could be derived for increasing chain length. One important reason for this may be that the molecules are mainly planar and rather rigid on the surface, and thus do not exhibit a significant configurational entropy even for the longer chain lengths. Moreover, we observed only a very small number of points defects within ordered domains, which further implies that the number of molecules that are not in the full transconformation is negligibly small. This is remarkable, because one could have expected a larger concentration of molecules of alternative conformations for several reasons. First, as mentioned above the energetic barriers for rotations around the thiophene-thiophene bonds are small ($\approx$5 kJ mol^{-1}) as shown by our semiempirical quantum-mechanical calculations, and molecules of different conformations could thus be expected for entropic reasons. Second, the molecules are not fully planar in the gas phase as shown from quantum-mechanical calculations[38] and experimental data.[46] Third, the molecules are presumably in a vibrationally and rotationally activated state when they are thermally evaporated onto the surface. From the fact that molecules with different conformations are *not* observed we may conclude that the adsorption process on the surface proceeds via a highly mobile intermediate state, which allows the molecules to adopt to their final optimal adsorption geometry and conformation. However, for such large molecules the dynamics of adsorption processes have not been investigated yet.

A high *lateral* mobility of adsorbed molecules on the surface is, of course, a prerequisite for the formation of long-range ordered domains. Our experiments thus demonstrate that the lateral corrugation of the bonding potential, (which is responsible for the lateral mobility) is small, albeit the molecules are very strongly bound to the surface. Since commensurate structures are observed only for the two smaller oligomers, we can further conclude that the lateral corrugation of the bonding potential is smaller for the longer molecules, although these are more strongly bound to the surface due to their larger π system. The obvious reason for this is that the lateral corrugation of the potential—and consequently the site-specific bonding—is smaller, the larger the number of thiophene units is. This finding is encouraging because it suggests that even larger molecules of this or of a similar type will form long-range ordered superstructures on Ag(111), which might appear as contraintuitive at first glance.

We further discuss the 2D geometric ordering that is observed as a function of the chain lengths of the oligomers. Obviously, the large exothermic adsorption energy strongly favors the lateral order, because this optimizes the density of molecules in the monolayers. In principle the adsorption energy causes a compression of the layers, which is compensated at small intermolecular distances by repulsive lateral intermolecular forces. On top of this more subtle effects due to the molecular symmetry, the molecular size, and the lateral corrugation of the substrate are relevant for the details of the geometric structures. From the here-obtained results it is tempting to postulate more general rules that predict the type of geometric structures that are formed on Ag(111) by ECnT's or by other similar molecules as a function of chain length, or more generally as a function of the molecular symmetry. A *first* rule would state that primitive unit cells will only be formed for molecules with an even number of thiophene units or C_{2h} symmetry. The *second* rule says that stacking structures are most likely formed in the compressed phases. However, EC4T is already an exception to this rule (see Fig. 6). A possible reason is that the compressed structure of EC4T is only *uniaxially* incommensurate and that it is thus strongly influenced by the substrate corrugation and much less by the intermolecular forces. This is also supported by the finding that the coverage of a hypothetical stacking structure of EC4T is about 5% larger than that of the observed structure. In this context we also note that EC4T forms a stacking structure on the more open Ag(110) surface,[16,47] which indicates that this structure is generally possible. From the above-postulated rules one could predict further structures, e.g., an analogous structure as that of EC5T is also expected for EC7T.

Finally, we consider the azimuthal orientation of the molecular layers on the substrate, which is described by the angle ϕ (cf. Fig. 7). For the two commensurate phases the orientation is a direct consequence of the energetically preferred adsorption site. The commensurability has the consequence that all lattice points of the adsorbate fall onto lattice points of the substrate surface. For the incommensurate structures the situation is more complicated and several different theoretical concepts have been developed to explain the azimuthal orientation. Hoshino *et al.* could explain the azimuthal orientation of monolayers of larger condensed aromates on the basal plane of graphite by the so-called *point-on-line concept*, which postulates a low interface energy for the case where all lattice points of the adsorbate fall onto one set of lattice lines of the substrate.[10] However, this concept does not allow the interpretation of the azimuthal orientations observed here. Furthermore, Forrest and Zhang have performed intensive computational modeling of the adsorption geometry of large condensed aromatic molecules on the basal plane of graphite.[48] Two main outcomes of their calculations are (i) that a large stiffness within the monolayer (intralayer stiffness) and a small interlayer shear stress (at the substrate/organic interface) are decisive for the long-range order in the monolayers, and (ii) that the azimuthal orientation of the adsorbate layer is given by the minimum of the interface energy of the rigid adsorbate layer with the substrate. Since in the present case the adsorbate/substrate interaction is considerably stronger than on graphite, we expect that the corrugation of the surface potential is also stronger and that intralayer stress is thus important, too, in contrast to the situation investigated by Forrest and Zhang.[48]

For the case of incommensurate monolayers of physisorbed inert gas atoms (with a small misfit with respect to the substrate) McTague and Navaco developed a model in this direction.[49] It predicts the azimuthal orientation from the minimization of longitudinal stress and shear stress within the adsorbate layer.[49] We suppose that a model of this kind will be adequate for the present situation, if in addition the strongly anisotropic molecules and the probably strongly structured local bonding potentials of the molecules to the substrate are included. In the present case we have some evidence for the importance of such a local surface/molecule bonding potential, since we find for all incommensurate structures a very similar orientation of the long molecular axis, namely, along the (1, 7.3) direction (cf. Fig. 6). At present we can only speculate about the reason for this specific orientation of the molecules. Possibly this orientation is energetically favored, because it yields a local commensurability of the periodic *internal* structure of the molecule that is related to the thiophene rings and the substrate. Therefore, we have to conclude that a theoretical understanding of the here-found adsorption geometries requires models that are more complicated than those presently used, which is to some extent due to the considerable corrugation of the substrate because of the covalent bonding.

VI. SUMMARY AND CONCLUSIONS

The adsorption and ordering behavior of four end-capped oligothiophenes of different chain lengths ($n=3-6$) on the Ag(111) surface was investigated by TPD, LEED, and STM. All oligomers adsorb on the surface with a coplanar orientation and form long-range ordered structures. In contrast to the situation present on inert substrates, e.g., graphite, the surface bonding is covalent and strong, thus preventing monolayer molecules from thermal desorption. From TPD we suppose that a layer-by-layer growth occurs, at least for the first three layers, and that the second layer is slightly stronger bound compared to further layers.

At saturation coverage of the first layer all oligomers form incommensurate (compressed) structures. In addition, commensurate superstructures are observed for EC3T and EC4T at 7–9 % smaller coverages. These commensurate-incommensurate phase transitions are fully reversible and can be achieved by thermal desorption or additional deposition of molecules. The additional formation of commensurate superstructures by the two shorter molecules is a clear indication for a site-specific bonding due to the lateral corrugation of the substrate. For the two longer oligomers of the series, which form only incommensurate structures, the site-specific bonding is obviously less relevant due to the larger number of Ag atoms the molecules are bound to. Remarkably, all incommensurate structures (with the exception of EC4T) exhibit a stacking structure with an identical orientation of the stacks. This specific azimuthal ordering of the adsorbate layer cannot be explained by the point-on-line concept, which was successfully used for organic monolayers on graphite, but possibly by an energetically preferred azimuthal orientation of the individual ECnT molecules with respect to the Ag(111) surface.

Our experiments clearly demonstrate that even for larger (suitable) oligomers, highly ordered superstructures can be achieved on the Ag(111) surface. This is meaningful because of several reasons. First, the preparation and structural investigation of organic monolayers on Ag(111) may serve as an additional technique to identify or control the geometric structures of new synthesized molecules. Second our results point out that the Ag(111) surface, or thin Ag films with (111) terraces, are attractive (conducting) substrates for the preparation of organic films by vapor deposition, since at least the interface, i.e., the first monolayer on the metal, is structurally well defined. Possibly the lateral order induced in the monolayer may be preserved also in further layers yielding epitaxial growth.[21]

ACKNOWLEDGMENTS

The authors wish to thank Professor H.-P. Steinrück, Professor W. Moritz, and Professor N. V. Richardson for fruitful discussions. This project was financially supported by the Bundesministerium für Bildung, Wissenschaft und Forschung through Project No. 05 BM 290/2. One of us (E.U.) gratefully acknowledges financial support by the Fond der Chemischen Industrie.

*Author to whom correspondence should be addressed. FAX: +49-931-888-5158.

Electronic address: moritz@miro.physik.uni-wuerzburg.de

[1] B. N. J. Persson, Surf. Sci. Rep. **15**, 1 (1992).

[2] A. Zangwill, *Physics at Surfaces* (Cambridge University Press, Cambridge, England, 1988).

[3] B. G. Frederick, F. M. Leibsle, S. Haq, and N. V. Richardson, Surf. Rev. Lett. **3**, 1523 (1996).

[4] T. J. Schuerlein and N. R. Armstrong, J. Vac. Sci. Technol. A **12**, 1992 (1994); A. Schmidt, T. J. Schuerlein, G. E. Collins, and N. R. Armstrong, J. Phys. Chem. **99**, 11 770 (1995).
[5] E. Umbach, C. Seidel, J. Taborski, R. Li, and A. Soukopp, Phys. Status Solidi B **192**, 389 (1995); E. Umbach, M. Sokolowski, and R. Fink, Appl. Phys. A: Mater. Sci. Process. **63**, 565 (1996).
[6] C. Seidel, A. Soukopp, R. Li, P. Bäuerle, and E. Umbach, Surf. Sci. **374**, 17 (1997).
[7] M. Bässler, R. Fink, C. Heske, J. Müller, P. Väterlein, J. U. von Schütz, and E. Umbach, Thin Solid Films **284**, 234 (1996).
[8] M. Möbus, N. Karl, and T. Kobayashi, J. Cryst. Growth **116**, 495 (1992).
[9] C. Ludwig, B. Gompf, W. Glatz, J. Petersen, W. Eisenmenger, M. Möbius, U. Zimmermann, and N. Karl, Z. Phys. B **86**, 397 (1992).
[10] A. Hoshino, S. Isoda, H. Kurata, and T. Kobayashi, J. Appl. Phys. **76**, 4113 (1994).
[11] J. E. Freund, M. Edelwirth, P. Kröbel, and W. Heckl, Phys. Rev. B **55**, 5394 (1997).
[12] S. Cincotti and J. P. Rabe, Appl. Phys. Lett. **62**, 3531 (1993).
[13] P. Bäuerle, Adv. Mater. **4**, 102 (1992).
[14] The series of unsubstituted oligothiophenes (αnT) exhibits C_{2v} and C_{2h} symmetry for $n=$odd and $n=$even, respectively. However, for the series of ECnT the symmetry is reduced by the nonplanar conformation of the terminal cyclohexene rings containing four sp^3-hybridized C atoms. Thus the highest possible symmetries are (depending on the relative conformation of the two cyclohexene rings) C_2 or C_S for $n=$odd and C_2 or C_i for $n=$even. At present, we do not know which conformations are present on the surface. However, we may expect that the symmetry groups of the planarized molecules C_{2v} and C_{2h} give good descriptions, because the nonplanarity of the end caps constitutes only a minor structural detail and only small additional structural distortions of the adsorbed molecules (with respect to the free molecules) are expected due to the weakness of the chemical bonding.
[15] A. Soukopp, Ch. Seidel, R. Li, M. Bässler, M. Sokolowski, and E. Umbach, Thin Solid Films **284–285**, 343 (1996).
[16] A. Soukopp, Ph.D. thesis, University of Würzburg, 1997.
[17] F. Garnier, R. Hajlaoui, A. Yassar, and P. Srivastava, Science **265**, 1684 (1994); A. Dodabalapur, L. Torsi, and H. E. Katz, *ibid.* **268**, 270 (1995).
[18] F. Geiger, M. Stoldt, H. Schweitzer, P. Bäuerle, and E. Umbach, Adv. Mater. **5**, 922 (1993); H. Neureiter, W. Gebauer, C. Väterlein, M. Sokolowski, P. Bäuerle, and E. Umbach, Synth. Met. **67**, 173 (1994).
[19] K. Uchiyama, H. Akimichi, S. Hotta, H. Noge, and H. Sakaki, Synth. Met. **63**, 57 (1994); G. Horowitz, P. Delannnoy, H. Bouchriha, F. Deloffre, J.-L. Fave, F. Garnier, R. Haijlaoui, M. Heyman, F. Kouki, P. Valat, V. Wintgens, and A. Yassar, Adv. Mater. **6**, 752 (1994).
[20] W. Gebauer, M. Bäßler, A. Soukopp, C. Väterlein, R. Fink, M. Sokolowski, and E. Umbach, Synth. Met. **83**, 227 (1996).
[21] W. Gebauer, M. Bäßler, R. Fink, M. Sokolowski, and E. Umbach, Chem. Phys. Lett. **266**, 177 (1997).
[22] E. Umbach, W. Gebauer, A. Soukopp, M. Bäßler, and M. Sokolowski, J. Lumin. **76**, 641 (1998).
[23] E. R. Frank, X. X. Chen, and R. J. Hamers, Surf. Sci. Lett. **334**, L709 (1995).
[24] M. B. Nardelli, D. Cvetko, V. De Renzi, L. Floreano, R. Gouter, A. Morgante, M. Peloi, F. Tommasini, R. Danielli, S. Rossini, C. Taliani, and R. Zamboni, Phys. Rev. B **53**, 1095 (1995).
[25] A. Soukopp, K. Glöckler, P. Bäuerle, M. Sokolowski, and E. Umbach, Adv. Mater. **8**, 902 (1996).
[26] P. Väterlein, Ph.D. thesis, University of Würzburg, 1997.
[27] M. Bäßler, Ph.D. thesis, University of Würzburg, 1997.
[28] A. Soukopp, K. Göckler, M. Sokolowski, and E. Umbach (unpublished).
[29] K. Besocke, Surf. Sci. **181**, 145 (1987).
[30] K. Glöckler, C. Seidel, A. Soukopp, M. Sokolowski, E. Umbach, M. Böhringer, R. Berndt, and W.-D. Schneider, Surf. Sci. **405/1**, 1 (1998); M. Böhringer, W.-D. Schneider, R. Berndt, K. Glöckler, M. Sokolowski, and E. Umbach, Phys. Rev. B **57**, 4081 (1998).
[31] PCMODEL, Molecular Modeling Software for the IBM PC/XT/AT and Compatibles (Version 3.0), Serena Software, Box 3076, Bloomington, IN 47402-3076.
[32] J. J. P. Stewart, MOPAC, Vers. 6.0, Quantum Chemistry Program Exchange, QCPE #455, Department of Chemistry, Indiana University, Bloomington, IN.
[33] L. Pauling, *The Nature of the Chemical Bond and the Structure of Molecules and Crystals* (Cornell University Press, Ithaca, NY, 1948).
[34] Molecular Simulations Inc., 9685 Scranton Road, San Diego, CA 92121-3752.
[35] A. K. Rappé, K. S. Colwell, and C. J. Casewit, Inorg. Chem. **32**, 3438 (1993).
[36] A. Soukopp, Diploma-thesis, University of Stuttgart, 1992.
[37] Here we assume C_2 symmetry for the even numbered ECnT and C_s symmetry for the odd numbered ECnT. Otherwise the space-group is lower, e.g., only $p1$ for EC4T (Ref. 6). See also Ref. 14. Note that the space group refers to the ''free-floating'' adsorbate layer only, since the glide planes are not symmetry elements of the substrate lattice. For the $p1g1$ and $p2gg$ space groups we have also neglected the small deviations of the unit cell from a *rectangular* unit cell, i.e., the small deviation of γ from 90° (cf. Table I).
[38] E. Mena, M. Sokolowski, P. Bäuerle, and E. Umbach (unpublished).
[39] D. A. King, Surf. Sci. **47**, 384 (1975); J. T. Yates, Jr., Methods Exp. Phys. **22**, 425 (1985); D. Menzel, in *Interaction on Metal Surfaces*, edited by R. Gomer (Springer, New York, 1975).
[40] E. Habenschaden and J. Küppers, Surf. Sci. **138**, L147 (1984).
[41] We note that E_{sub} is the averaged adsorption energy per molecule in the *incommensurate* (compressed) phase.
[42] We note that the bulk structures of the end-capped oligothiophenes are unknown.
[43] W. Huber, P. Zebisch, T. Bornemann, and H.-P. Steinrück, Surf. Sci. **258**, 16 (1991).
[44] O. Böhme, C. Ziegler, and W. Göpel, Adv. Mater. **6**, 587 (1994).
[45] C. Mainka, P. S. Bagus, A. Schertel, T. Strunskus, M. Grunze, and Ch. Wöll, Surf. Sci. **341**, L1055 (1995).
[46] A. Gavezzotti and G. Fillippini, Synth. Met. **40**, 257 (1991).
[47] A. Soukopp, K. Glöckler, P. Bäuerle, M. Sokolowski, and E. Umbach (unpublished).
[48] S. R. Forrest and Y. Zhang, Phys. Rev. B **49**, 11 297 (1994).
[49] J. P. McTague and A. D. Navaco, Phys. Rev. B **19**, 5299 (1979).